

## Sink strength simulations using the Monte Carlo method: applied to spherical traps

T. Ahlgren\*, L. Bukonte\*

*Department of Physics, University of Helsinki, P.O. Box 43, FI-00014 Helsinki, Finland*

---

### Abstract

The sink strength is an important parameter for the mean-field rate equations to simulate temporal changes in the micro-structure of materials. However, there are noteworthy discrepancies between sink strengths obtained by the Monte Carlo and analytical methods. In this study, we show the reasons for these differences. We present the equations to estimate the statistical error for sink strength calculations and show the way to determine the sink strengths for multiple traps.

We develop a novel, very fast Monte Carlo method to obtain sink strengths. The results show that, in addition to the well-known sink strength dependence of the trap concentration, trap radius and the total sink strength, the sink strength also depends on the defect diffusion jump length and the total trap volume fraction. Taking these factors into account, allows us to obtain a very accurate analytic expression for the sink strength of spherical traps.

---

### 1. Introduction

To understand and control the changes in the physical and mechanical properties of materials during ageing or ion irradiation, requires a long time and length scale simulation technique, knowledge of the ion irradiation produced defects, and a complete description of how the formed defects diffuse and interact with each other.

The only simulation techniques that are able to fulfil the long time and length scales are the mean-field rate equations (RE) and kinetic Monte Carlo (KMC) methods. The KMC is a stochastic simulation method, where all the dynamic properties and reactions for all involved defects have to be known. The strengths of this method include the ability to take into account expected and unexpected correlated events, e.g. close Frenkel pair annihilation. However, the time step for the KMC method is inversely proportional to the sum of frequencies of all processes, which is a disadvantage in some cases. For instance in tungsten, where the self-interstitial atom moves very fast [1], the KMC time step, even with only one SIA present, might be of the order of  $10^{-11}$  s. Clearly, this restricts the accessible time and defect concentrations for the method.

---

\*Corresponding author. Department of Physics, University of Helsinki, P.O. Box 43, FI-00014 Helsinki, Finland  
Email address: [tommy.ahlgren@helsinki.fi](mailto:tommy.ahlgren@helsinki.fi) (T. Ahlgren)

In the mean-field rate equations (RE) [2, 4, 5] the defects and other objects are treated as concentrations (number/vol) which interact with each other in space and time. This interaction is described by a parameter called the sink strength, which determines the probability for mobile defects to interact with any other point or extended defect in the material. The sink strength has to be determined for each mobile defect separately and it is proportional to the square of the inverse mean distance covered by the defect before it is absorbed, trapped or annihilated. The sink strength is the single most important parameter in RE simulations and is a function of the geometry, size and concentration of sinks, dimensionality of the diffusion, and, as we will show in this study, the sink strength also depends on the diffusion jump length of the defect.

Sink strengths have been determined for various symmetric traps including spherical traps, dislocation lines and loops, and grain boundaries [6, 7, 8, 9]. Monovacancies, vacancy clusters, self-interstitial atoms and impurities are usually counted as spherical traps. For arbitrarily shaped traps, methods like the Monte Carlo (MC) method has to be used to determine the sink strength. The MC method seems in principle straight forward to use, but previous studies have shown some inconsistencies for this method. Malerba *et al.* [7] have noticed that the MC method gives smaller sink strengths than the analytic equation for spherical traps in the low trap volume fraction region. On the contrary, for large trap volume fractions, the sink strengths simulated by the MC method are much larger than the analytical ones. Similar results are observed by Hou *et al.* [10], where the analytic equation is modified to give better agreement with the sink strengths obtained by the MC method.

In this study, we show the reasons for the discrepancy between sink strengths obtained analytically and by MC. We introduce a new, much faster MC concept to simulate sink strengths. We further show how the equation of analytical sink strength can be modified so that it can be used in defect and micro structure simulations with any trap volume fraction and defect jump length.

## 2. Results

The definition of the sink strength includes the inverse mean distance squared a defect diffuses before it gets trapped. The sink strength calculated with the Monte Carlo (MC) method is expressed as [11]:

$$k^2 = \frac{2 \cdot Dim}{\lambda^2 \langle N \rangle}, \quad (1)$$

where  $Dim$  is the dimension for the defect diffusion,  $\lambda$  is the jump length and  $\langle N \rangle$  is the mean number of jumps the defect makes before it is trapped:  $\langle N \rangle = \sum_{i=1}^M N_i / M$ , where  $M$  is the number of defects simulated and  $N_i$  is the number of defect  $i$  jumps before it is trapped. In Appendix A, we show how the statistical error for determining the sink strength by the MC method depends on the number of defects  $M$  simulated as follows:

$$\Delta k^2 = k^2 \frac{\sqrt{\sum_{i=1}^M (1 - N_i / \langle N \rangle)^2}}{M} \approx \frac{k^2}{\sqrt{M}}. \quad (2)$$

As a rule of thumb, to obtain the sink strength with an error less than 1% more than  $10^4$  defects need to be simulated, and for an error less than a per mille (1 ‰) more than  $10^6$  defects are needed, see Fig. A.10.

In this study, we place one trap in the middle of the simulation cell, which is either spherical or cubic. The trap concentration  $c_t$  is controlled by choosing an appropriate simulation cell volume  $V$ ,  $c_t = 1/V$ . The trap volume fraction becomes:  $VF_t = 4\pi R_t^3/(3V)$ . One defect at a time is placed at a random position in the cell, excluding the trap volume. The defect diffusion jumps are counted until it jumps inside the trapping radius  $R_t$ , then a new defect is inserted in the cell. At least  $M = 10^6$  defects are simulated for each sink strength calculation, resulting in the statistical error of about 1 ‰.

### 2.1. Improving MC sink strength simulation speed

The MC method for determining the sink strength of systems with quite small trap volume fractions is very inefficient [7]. The reason for this is that the defect can make incredibly large number of jumps before it finds a trap ( $k^2 = 6/[\langle N \rangle \lambda^2]$ ), see Eq. (1). Thus, to find the sink strength for a trap with, let's say, a trap radius  $R_t = 0.4$  nm and concentration of  $c_t = 10^{-7} \text{ nm}^{-3}$  ( $k^2 \approx 4\pi c_t R_t$ ), for a statistics of  $10^6$  defects, with jump length  $\lambda = 0.1$  nm, we would need about  $10^6 \cdot 6/(4\pi 10^{-7} 0.4 \cdot 0.1^2) \approx 10^{15}$  jumps.

In this study, we develop a new and fast MC method to simulate sink strengths, the details are given in Appendix B. The method takes advantage of the fact that if the minimum distance to any trap for the diffusing defect is known (this has to be checked anyway during the MC simulation), the defect cannot be trapped during the following  $N^j = \text{floor}(D_{min}/\lambda)$  diffusion jumps, where  $D_{min}$  is the minimum distance to any trap and  $\lambda$  is the jump length. Thus, instead of making  $N^j$  diffusion jumps, we can make one jump that gives statistically the same diffusion distance as the  $N^j$  individual diffusion jumps would give. This new concept gives surprisingly large improvement in the simulation times. To compare the normal MC with the new (*N-jump*) MC method, we determine the average cpu-time per defect during sink strength simulations for seven different trap volume fractions  $VF_t$ :  $10^{-1}$ ,  $10^{-2}$ ,  $10^{-3}$ ,  $10^{-4}$ ,  $10^{-5}$ ,  $10^{-6}$  and  $10^{-7}$ . The trapping radius  $R_t$  is 0.5 nm for all simulations. Two different jump lengths  $\lambda = 0.2$  and 0.005 nm are chosen for every simulation. The choice of the latter very small jump length will be obvious in the next section where we compare the MC results with analytical sink strengths. Figure 1 shows the impressive improvement in the simulation times for the *N-jump* MC method. For rather large trap volume fractions  $VF_t$  above  $10^{-3}$  and jump length to trapping radius ratio  $\lambda/R_t = 0.4$ , both methods give similar simulation times. This is expected because the distance to the closest trap is never very large, thus the *N-jump* MC method is seldomly used. However, for smaller trap volume fractions the improvement in simulation time is remarkable. Smaller  $\lambda$  to  $R_t$  ratio yields to even more impressive improvement in computational times. For  $\lambda$  to  $R_t$  ratio of  $5 \times 10^{-3}$ , the *N-jump* MC method is faster for all trap volume fractions, being a staggering more than four orders of magnitude faster at  $VF_t = 10^{-7}$ . The new method enables sink strength simulations for smaller trap volume fractions with better statistics. The resulting sink strengths for both normal and *N-jump* MC methods are the same within the statistical error. All the following sink strengths in

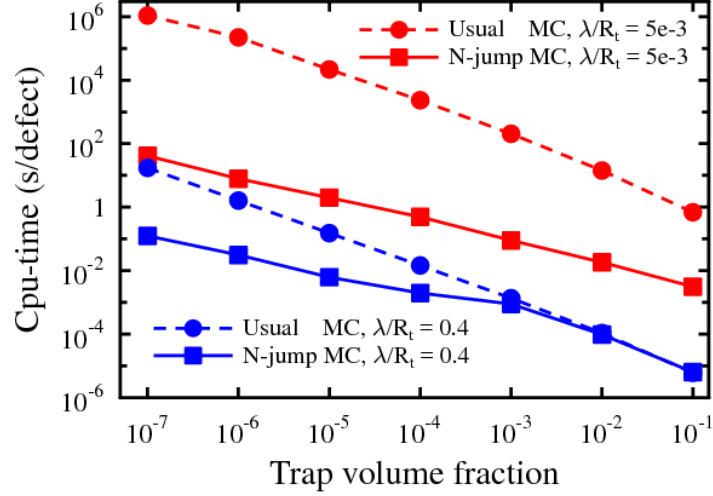


Figure 1: Comparison of cpu-time per defect for the usual and the developed *N-jump* MC methods for two different jump length to trapping radius ratio and trap volume fractions between  $10^{-7}$  -  $10^{-1}$ . The lines are given as guides to the eye.

this study have been calculated with the developed *N-jump* MC method.

## 2.2. Comparison of the analytical and MC sink strengths

The analytical sink strength for spherical traps under 3D diffusion limit with trap radius  $R_t$  and concentration  $c_t$  is given by the recursive equation by Brailsford and Bullough [6]:

$$k^2 = 4\pi R_t c_t (1 + R_t \sqrt{k^2}). \quad (3)$$

In the small trap concentration limit the Eq. (3) is usually truncated to the first order ( $n = 1$ ),  $k^2 = 4\pi R_t c_t$ . For usual trap concentrations higher order sink strengths ( $n = 2, 3, 4, \dots$ ) are calculated recursively as  $k_n^2 = 4\pi R_t c_t (1 + R_t \sqrt{k_{n-1}^2})$ . For  $n = \infty$  the solution can be found directly from Eq. (3) as  $k^2 = \left(2\pi R_t^2 c_t [1 + \sqrt{1 + 1/(\pi R_t^3 c_t)}]\right)^2$ . In the case of many traps, the sink strength in the square root of Eq. (3) is the sum of all the sink strengths. The derivation of the analytical sink strength above assumes spherically symmetric cell and much smaller jump length than the trap radius [6]. Therefore, in our MC method we also use spherical symmetry by reflecting back the defect when it jumps past the spherical simulation cell radius. The small jump length criteria is tested by simulating the sink strength as a function of jump length for five different trap volume fractions  $V F_t$ :  $10^{-1}$ ,  $10^{-2}$ ,  $10^{-3}$ ,  $10^{-4}$  and  $10^{-5}$ , with two different trapping radii. Figure 2 shows the  $k^2$  decrease as a function of the jump length to trapping radius ratio ( $\lambda/R_t$ ). All the  $k^2$  values have been divided by the  $k^2$  value simulated using the smallest  $\lambda$ . Consequently the MC simulations will give smaller  $k^2$  than the analytic function if the jump length compared to the trap radius is not small enough. A similar decrease of the  $k^2$  values have already previously been observed [11, 7, 10]. Heinisch *et al.* [11] explain this decrease due to the discrete nature of the diffusion mechanism in which each defect jump is a fixed distance. Their correction formula

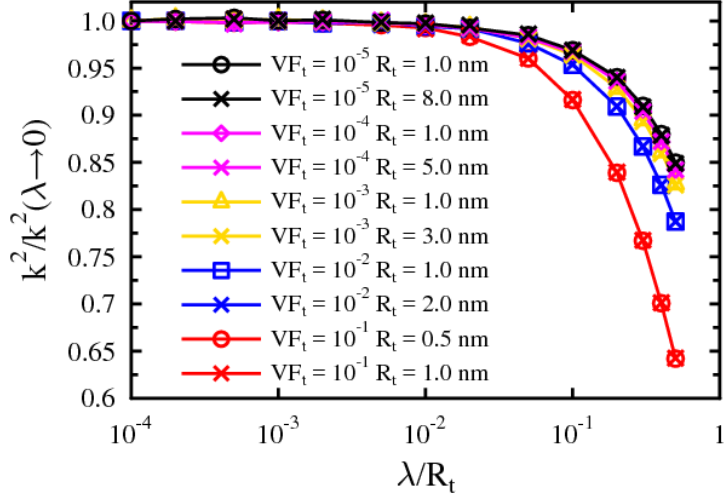


Figure 2: The decrease in the MC sink strength as a function of jump length  $\lambda$  to trap radius  $R_t$  ratio for different trap volume fractions  $VF_t$  and trap radii. For  $\lambda/R_t$  ratio smaller than about  $10^{-2}$  the  $k^2$  values do not change much anymore. Note that the decrease in the  $k^2$  values depend only on the trap volume fraction and on the  $\lambda/R_t$  ratio, and not on the trapping radius.

to the sink strength [11], will be compared in section 2.4. Hou *et al.* [10] have analyzed in more depth the small trap sink strength discrepancy. They have concluded that since the jump distance is not zero, the defects in MC simulations can penetrate into the sink. The authors have derived a correction term to the sink strength that depend on the trap radius and defect jump length, which also will be compared in section 2.4. Looking closer at Fig. 2, we see that the sink strength correction besides depending on the jump length to trap ratio, also depends on the trap volume fraction. In fact, any trap radius with a constant jump to trap ratio has the same  $k^2$  decrease for any fixed trap volume fraction. This suggests that a defect with smaller jump length  $\lambda$  (with the same diffusion distance squared:  $N\lambda^2$ ) explores its closest surrounding volume more thorough and finds traps with a shorter diffusion distance. This could also be the reason why the correction is larger for larger trap volume fractions.

To ensure that the small jump length criteria is fulfilled, we choose the jump length to trap radius ratio to be 1/1000 (see Fig. 2) for all the following MC simulations.

The discrepancy between the analytical and MC sink strengths at large trap volume fractions,  $VF_t$ , arises partly from the fact that the analytical result is derived for small trap volume fraction. To extend the theory approach to large  $VF_t$ , we revisit the sink strength theory in Appendix C. Including the trap volume in the mean defect concentration calculations, results in the following sink strength equation derived by Wiedersich [2, 3]:

$$k^2 = \frac{c_t [1 - R_t^3/L^3] 4\pi R_t}{\left[1 - 9R_t/(5L) + R_t^3/L^3 - R_t^6/(5L^6)\right]}, \quad (4)$$

where  $R_t$  and  $c_t$  are, as previously noted, the trap radius and the trap concentration, respectively, and  $L$  is the spherical cell radius. There is one trap in the center of the spherical cell, giving the trap concentration:  $c_t = 1/(4/3\pi L^3)$ .

Figure 3 compares the analytical sink strengths calculated by Eqs. (3) and (4) with the ones from MC simulations. The classical Eq. (3) result is calculated using the  $n = \infty$  solution. We can observe that all results agree for the smallest trap volume fractions. For larger trap volume fractions only the volume corrected analytic equation, Eq. (4), agrees with the MC results. To recap, the discrepancies between the sink strength theory and the MC simulations are removed if in the MC simulations the jump length compared to the trapping radius is small enough and a spherical simulation cell is used, and in the theory the trap volume fraction is taken into account. However, to simulate a real system, the boundary conditions are periodic (no spherical cell), and the jump length is given by the underlying lattice. Therefore a new and practical sink strength formulation is needed, that is presented in the following sections.

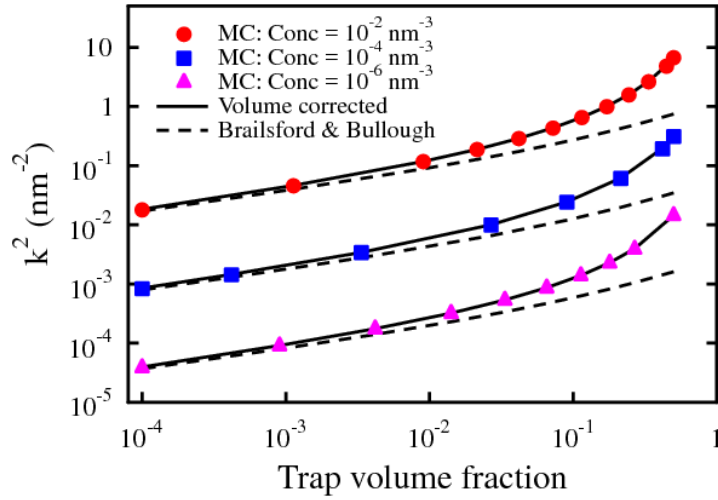


Figure 3: Analytical and MC sink strengths as a function of trap volume fractions. Eq. (4) agrees perfectly with the MC simulations throughout the whole trap volume fraction region. The presently accepted and widely used classical expression by Brailsford and Bullough, Eq. (3)  $n = \infty$  solution, consistently underestimates the sink strength and is about an order of magnitude too small for trap volume fraction of about 0.5.

### 2.3. Sink strengths with periodic boundary conditions

Next, the sink strengths are simulated with MC by placing one trap in the middle of a cubic simulation cell using periodic boundary conditions (a defect jumping outside the cell re-appears at the other side of the cell). As already noted, the jump length to trap radius ratio  $\lambda/R_t$  is chosen to be 1/1000 for all MC simulations. Figure 4 compares the results using a cubic and a spherical cell (see previous section) in the simulations. The sink strengths for the two different simulation cells agree for trap volume fraction below about  $10^{-2}$ . The reason for the larger  $k^2$  in the spherical cell case for large trap volume fractions is clear: when the defect crosses the boundary, it is, after the appropriate boundary condition, in most cases slightly closer to the central trap in the spherical cell case compared to the cubic cell. Shorter distance means less diffusion jumps before trapping, i.e. larger sink strength. For large simulation cells (small trap volume fractions) the difference becomes negligible as shown in Fig. 4.

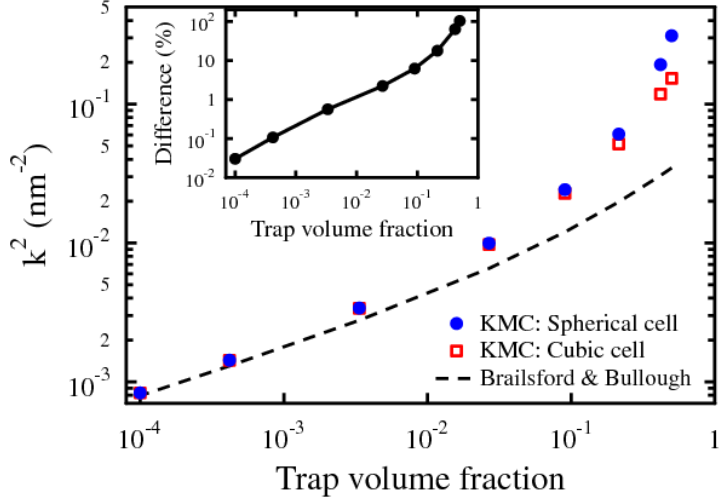


Figure 4: Sink strengths calculated by MC using either a cubic cell with periodic boundary condition or a spherical cell with reflective boundary condition. Shown is also the analytic expression by Brailsford and Bullough, Eq. (3). The inset shows the difference between the spherical and cubic cell results. The spherical cell gives more than 1% larger sink strengths than the cubic one for trap volume fractions larger than about 0.01.

Because the cubic and spherical cell simulations do not give the same sink strengths, Eq. (4) cannot be used. Moreover, Eq. (4) does not include the possibility to have more than one kind of trap in the system.

The following equation, modified from Eq. (3), describes the MC cubic box sink strength data accurately:

$$k^2 = 4\pi c_t R_t \left[ 1 + \alpha \cdot R_t \sqrt{k_{tot}^2} \right] \exp(\beta \cdot VF_{tot}^\gamma), \quad (5)$$

where  $R_t$  and  $c_t$  are the trap radius and trap concentration, respectively,  $k_{tot}^2 = \sum_j k_j^2$  is the sum of all sink strengths and  $VF_{tot} = \sum_j VF_j$  is the sum of all trap volume fractions. The fitting parameters are:  $\alpha = 0.6812067$ ,  $\beta = 1.3821147$  and  $\gamma = 0.3238967$ . Figure 5 confirms that this relatively simple equation accurately fits the MC data.

To convince ourselves that Eq. (5) is quite general, it is compared to simulations where we have two different traps simultaneously. Trap A,  $R_t = 3$  nm, with a constant concentration of  $10^{-4}$  traps/nm<sup>3</sup>, and trap B,  $R_t = 2$  nm, with increasing concentration from  $10^{-5}$  to  $5 \times 10^{-3}$  traps/nm<sup>3</sup>. The jump length  $\lambda$  is 0.002 nm and the number of defects simulated in each case is  $2 \times 10^6$ .

The MC sink strength for each trap type  $j$  becomes:

$$k_j^2 = \frac{2 \cdot Dim}{\lambda^2 N / M_j}, \quad (6)$$

where  $N = \sum_{i=1}^M N_i$  is the sum of the jumps all the  $M$  number of defects make until they are trapped in any trap, and  $M_j$  is the number of defects trapped in trap type  $j$ . Note that  $M = \sum_{j=1}^Q M_j$ , where  $Q$  is the number of different traps. From this definition, we see that the total sink strength is the sum of all sink strengths:  $k_{tot}^2 = \sum_{j=1}^Q k_j^2 = \frac{2 \cdot Dim}{\lambda^2 N} \sum_{j=1}^Q M_j = \frac{2 \cdot Dim}{\lambda^2 N / M} = \frac{2 \cdot Dim}{\lambda^2 \langle N \rangle}$ . Figure 6 shows that Eq. (5) also gives the sink strengths for multiple traps. Note how the sink strength

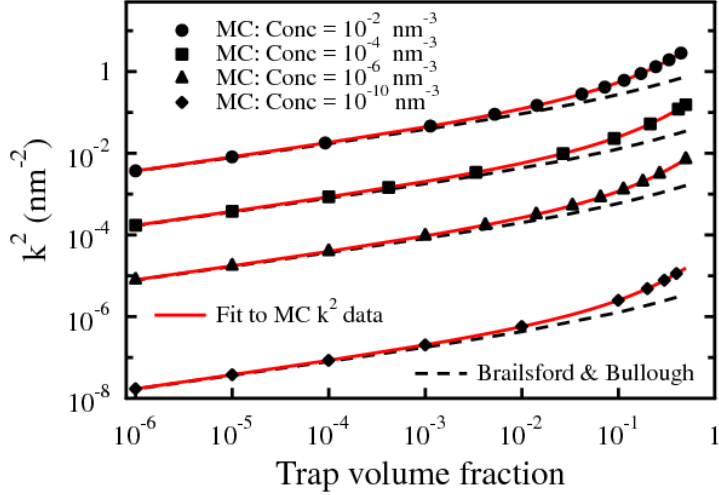


Figure 5: MC sink strengths as a function of trap volume fractions and concentrations for cubic cell using periodic boundary conditions. The solid line is the fit given by Eq. (5) and the dashed line is the classical expression by Brailsford and Bullough, Eq. (3).

for trap A (with constant concentration) increases due to the other trap B. The classical expression by Brailsford and Bullough, Eq. (3) is determined with  $n = 10$  recursive iterations. The trap volume fractions are quite high ( $> 0.01$ ) which is the reason why the Brailsford and Bullough approach does not work so well.

The slight overestimation of the sink strengths by Eq. (5) compared to the MC simulations most likely arises from the fact that the equation is fitted to a trap system where the traps are located at a maximum distance from each other (a cubic system with one trap in the middle with periodic boundary conditions). In reality and in the case of the two trap MC simulations, the traps are distributed randomly in the simulation cell. Thus, the distance between the traps is not constant but varies from the possible minimum of two times the trap radius to the theoretical maximum of the cell size. When defects are inserted randomly in the simulation cell the individual number of jumps  $N_i$  for the defects to be trapped changes. In case the defect happens to be initially placed in a locally higher trap concentration region, it makes fewer diffusion jumps before it is trapped, compared to a defect initially located in a lower trap concentration region. However, the mean increased number of jumps for defects in lower trap concentration region is larger than the mean decrease in the number of jumps in a region with higher trap concentration. The result is that the sum number of jumps  $N = \sum_{i=1}^M N_i$  is higher for systems with varying trap distances compared to the equidistant trap system, giving a slightly smaller sink strength in the varying trap distance case. This effect, judging from Fig. 6, is relatively small making Eq. (5) an accurate estimation.

#### 2.4. Sink strengths for a system with periodic boundary conditions for any jump length

The simulation of a real system has to deal with the defect diffusion jump length that is given by the underlying lattice. Therefore, we have to determine the way to correct the sink strength, Eq. (5), calculated with a very small



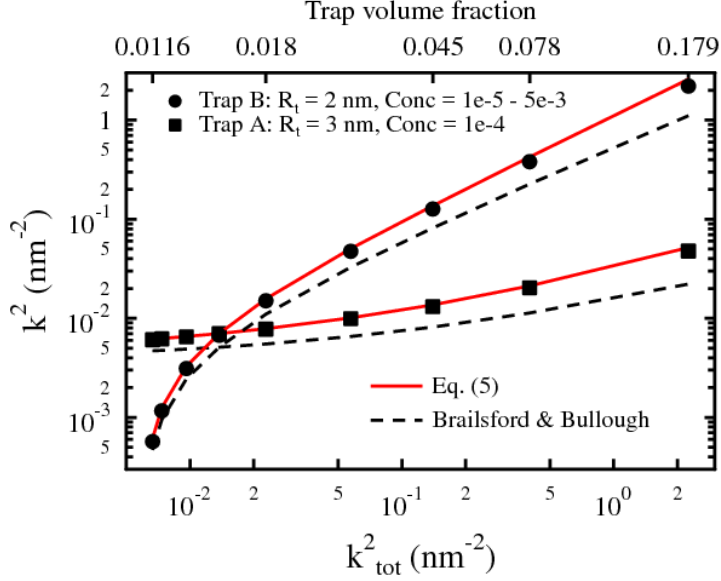


Figure 6: Analytical and MC sink strengths for a two-trap system with constant concentration for trap A and increasing concentration for trap B. Eq. (5), solid line, agrees fairly well with the simulations. The classical expression by Brailsford and Bullough, Eq. (3), is shown by dashed lines.

jump length, to sink strengths with any jump length. This is done in a similar way as in the earlier section where the sink strengths are simulated by MC as a function of jump lengths for different trap volume fractions. In this case, we use periodic boundary conditions and a cubic simulation cell. The number of defects simulated for each jump length is  $10^6$ . The results show, like in section 2.2, that the larger the jump length divided by trapping radius is, the smaller is the resulting sink strength. The following equation is observed to reproduce the MC results:

$$\frac{k^2(\lambda)}{k_{\lambda \rightarrow 0}^2} = \exp\left(\frac{-A \cdot \lambda/R_t}{1 - B \cdot VF_{tot}^C}\right), \quad (7)$$

where  $k^2(\lambda)$  is the sink strength given by any jump length  $\lambda$  and  $k_{\lambda \rightarrow 0}^2$  is the sink strength calculated by the smallest jump length to trapping radius ratio ( $\lambda/R_t = 10^{-4}$ ). The three fitting parameters are:  $A = 0.299299$ ,  $B = 1.180907$  and  $C = 0.251801$ . Figure 7 shows the decrease in the  $k^2(\lambda)/k_{\lambda \rightarrow 0}^2$  ratio as the  $\lambda/R_t$  ratio increases. We can see that for traps with small trap radius, for example, monovacancy where the  $\lambda/R_t$  ratio might be about 0.5, gives an approximate reduction of 15% in the sink strength for trap volume fractions up to about  $10^{-3}$ . For larger trap volume fractions the decrease in the sink strength values as a function of  $\lambda/R_t$  ratio is even more significant. Finally, the sink strength using arbitrary jump length and trap volume fractions, is given by combining Eqs. (5) and (7), where  $k_{\lambda \rightarrow 0}^2$  in Eq. (7) is given by  $k^2$  in Eq. (5). To compare the existing analytical sink strengths with the sink strengths obtained in this study, Eqs. (5) and (7), we simulate sink strengths for spherical traps with different trap volume fractions and trap radii. The defect jump length is 0.112 nm and number of defects is  $2 \times 10^6$  for all the simulations with cubic box and periodic boundary conditions. Figure 8 shows the percentage error,  $100 \times (k^2(\text{analytical}) - k^2(\text{MC}))/k^2(\text{MC})$ ,

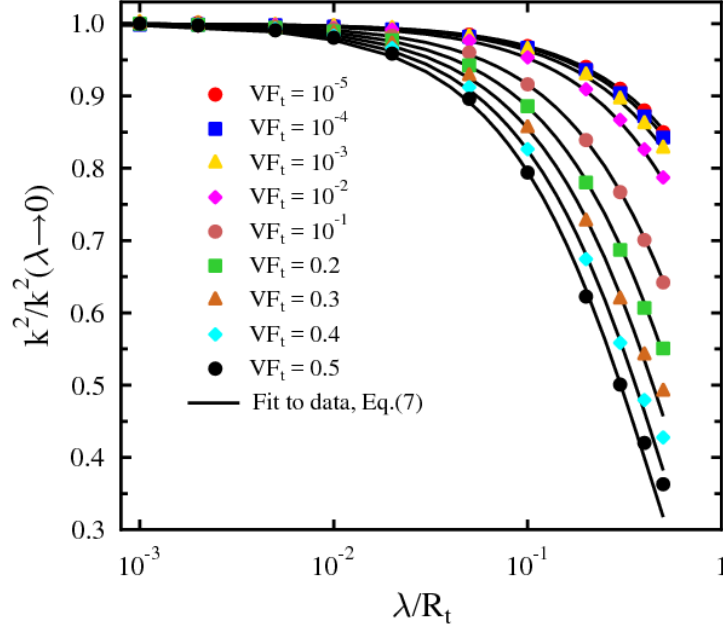


Figure 7: The fraction of sink strength with variable jump length to sink strength calculated with jump length divided by  $R_t$  equal to  $10^{-4}$ . The sink strengths by MC are given by markers. Eq. (7), solid lines, agrees well with the MC data.

for all the analytic equations. The equations presented in this study, Eqs. (5) and (7), show nearly zero error, while the commonly used recursive equation by Brailsford and Bullough [6], Eq. (3) with  $n = \infty$  recursion, overestimates the sink strength by more than 10% for small trap radius of  $R_t = 0.274$  nm, at trap volume fraction  $10^{-6}$ . For large trap volumes fractions close to 0.1, the Brailsford and Bullough equation underestimates the sink strength by about 30% for all trap radii. The analytic equation proposed by Hou *et al.* [10] shows improved accuracy compared to Brailsford and Bullough at small trap volume fractions, but still underestimates the sink strength substantially for large trap volumes fractions, as seen in Fig. 8. The correction formula, Eq. (2), by Heinisch *et al.* [11] (not plotted here) has larger negative errors than Hou *et al.* [10] equation in all the graphs in Fig. 8. To conclude, Eq. (7) should be used if the jump length to trap radius ratio is larger than about 0.01, which for a usual diffusion jump length of 0.1 nm means that the correction is needed for all traps with radii smaller than about 10 nm. The reason why the usually used Brailsford and Bullough (B&B) equation sometimes works well can be seen in Fig. 8 a) and b). In Fig. 8 a) the (B&B) equation has no error for trap radius 0.274 nm at trap volume fraction of about  $2 \times 10^{-3}$ . The jump length error that gives too large sink strength is exactly balanced by the trap volume fraction error that decreases the sink strength. In Fig. 8 b) this crossover happens for trap radius 1.0 nm at trap volume fraction of about  $2 \times 10^{-5}$ .

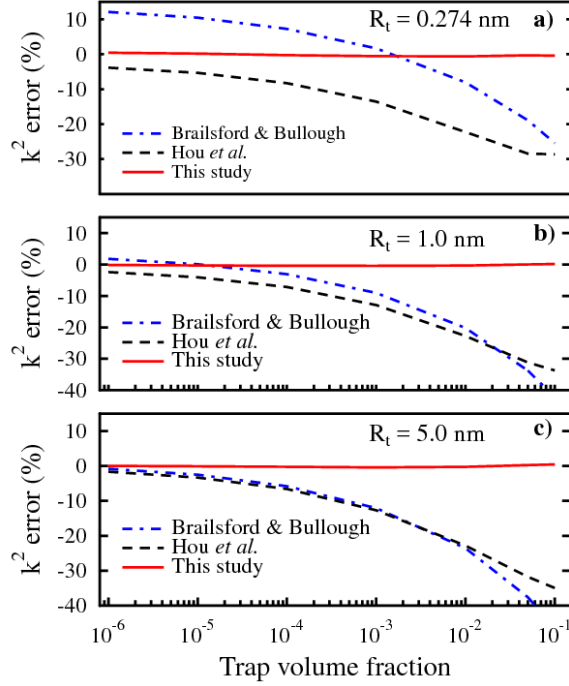


Figure 8: Errors for analytical sink strengths compared to MC data. This study refers to the combination of Eqs. (5) and (7).

### 3. Discussion

The results of this study show how to obtain reliable sink strength values that have far-reaching consequences for simulating defect dynamics with mean-field rate equations. As Fig. 8 shows, the commonly accepted and used sink strength values by Brailsford and Bullough [6] might be 10% too large for small trap volume fractions, and more than 30% too small for large trap volume fractions. Consequently, the results of the RE simulations are inevitably influenced by these large errors in the sink strengths.

Further, the observation that the MC sink strength is smaller than theory predicts at small trap volume fractions, and larger than given by theory at large trap volume fractions might be a quite general trend. Similar sink strength discrepancies have been observed by Jansson *et al.* [8] for dislocation sink strength simulations in the 1D case. This discrepancy can be partly explained by the results in this study: the quite large jump length affects the results for small trap volume fractions, and the trap volume starts to have an effect at large trap volume fractions.

Thus, it seems to be quite difficult to determine the sink strengths theoretically. For instance, in the spherical trap case the spherical simulation cell with reflective boundary conditions is not a good approximation for the correct cubic cell with periodic boundary conditions. To determine the analytical sink strength, like in Appendix C for a cubic system, needs a concentration solution in three dimensions, which anyway would lead to numerical approximations. Moreover, the relatively long defect jump length compared to usual point defect trapping radii, cannot easily be taken

into account in the theoretical approach.

Apparently the best way to obtain sink strengths seems to be using different MC methods, where the trap geometry, defect jump length and any simulation cell requirements are easily taken into account. Even the statistical error for the sink strength can now be estimated by Eq. (2). The MC method became more appealing now due to the *N-jump* MC method developed in this study. It takes sink strength simulations to a new level, with faster simulations statistics can be improved and sink strengths at smaller trap volume fractions become available. The *N-jump* method can be used to determine the sink strength for any kind of trap as long as the diffusion is three dimensional (3D). Further, it should be quite straight forward to extend the *N-jump* method to also cope with 1D and mixed 1D/3D diffusion with occasional direction changes.

#### **4. Conclusions**

We have now explained the reasons for the discrepancies between the sink strengths obtained with MC simulations and analytical studies. At low trap volume fractions, i.e., for small trap radii, the MC results are smaller than the analytical solution because of the large jump length compared to the trapping radius. For large volume fractions the explanation is twofold: firstly the analytic equation is derived for spherically symmetric cell, while the MC simulations are done for a cell with periodic boundary conditions. The second factor: the analytic expression is derived assuming small trap volume fraction. When the diffusion jumps, boundary conditions and the trap volume fraction is taken into account in the defect concentration, the sink strengths by the analytic and MC method show good agreement. We have presented a new method for much faster sink strength calculations with MC and showed a way to obtain the statistical error for the sink strengths. The developed *N-jump* method improves the statistical accuracy and opens possibilities to simulate sink strengths at lower trap volume fractions. The MC method can now also be used to determine the sink strengths for many traps simultaneously.

#### **Acknowledgements**

This work has been carried out within the framework of the EUROfusion Consortium and has received funding from the Euratom research and training programme 2014 - 2018 under grant agreement No 633053. The views and opinions expressed herein do not necessarily reflect those of the European Commission. Grants of computer time from the Centre for Scientific Computing in Espoo, Finland, are gratefully acknowledged.

## Appendix A. Statistical error estimate for sink strengths calculated by the MC method

The statistical error for the sink strength as a function of the mean number of jumps  $\langle N \rangle$  is obtained from Eq. (1) as:

$$\frac{dk^2}{d\langle N \rangle} = -\frac{2 \cdot Dim}{\lambda^2} \frac{1}{\langle N \rangle^2} \quad (\text{A.1})$$

$$\Rightarrow |\Delta k^2| = \frac{2 \cdot Dim}{\lambda^2} \frac{\Delta \langle N \rangle}{\langle N \rangle^2}, \quad (\text{A.2})$$

where the minus sign comes due to the fact that when  $\langle N \rangle$  decreases  $k^2$  increases.  $Dim$  is the dimension for the defect diffusion,  $\lambda$  is the jump length.  $\langle N \rangle = \sum_{i=1}^M N_i / M$ , where  $M$  is the number of defects simulated and  $N_i$  is the number of jumps the defect  $i$  makes before it is trapped. The usual standard deviation for the number of jumps is:

$$\Delta \langle N \rangle = \frac{\sqrt{\sum_{i=1}^M (\langle N \rangle - N_i)^2}}{M}, \quad (\text{A.3})$$

which, together with Eq. (A.2), gives the standard deviation statistical error for the sink strength:

$$\Delta k^2 = \frac{2 \cdot Dim}{\lambda^2} \frac{\sqrt{\sum_{i=1}^M (\langle N \rangle - N_i)^2}}{\langle N \rangle^2 M}. \quad (\text{A.4})$$

The term  $\sqrt{\sum_{i=1}^M (\langle N \rangle - N_i)^2}$  might become unmanageably large if  $N_i$  and  $M$  is large. An equivalent, but numerically friendlier form of Eq. (A.4) is:

$$\Delta k^2 = \frac{2 \cdot Dim}{\lambda^2} \frac{\sqrt{\sum_{i=1}^M (1 - N_i / \langle N \rangle)^2}}{\langle N \rangle M}. \quad (\text{A.5})$$

The error calculation for the sink strength is tested in Fig. A.9, where the sink strength  $k^2$  is determined with thousand different MC simulations with the same parameters. Figure A.9 b) shows that the error is described well by Eq. (A.5). The error or the standard deviation of the sink strength in Eq. (A.5) can also be written as a function of the sink strength, Eq. (1), as:

$$\Delta k^2 = k^2 \frac{\sqrt{\sum_{i=1}^M (1 - N_i / \langle N \rangle)^2}}{M} = k^2 \sqrt{\frac{\sum_{i=1}^M (1 - N_i / \langle N \rangle)^2}{M}} \frac{1}{\sqrt{M}}. \quad (\text{A.6})$$

The expression  $[\sum_{i=1}^M (1 - N_i / \langle N \rangle)^2] / M \approx 1$  in the square root term, giving a surprisingly simple rule to estimate the percentage error for simulated sink strengths as:

$$\frac{100 \Delta k^2}{k^2} = \frac{100}{\sqrt{M}}. \quad (\text{A.7})$$

To obtain sink strength with error less than 1% you need more than  $10^4$  defects, and for error less than a per mille (1‰) you need more than  $10^6$  defects, see Fig. A.10.

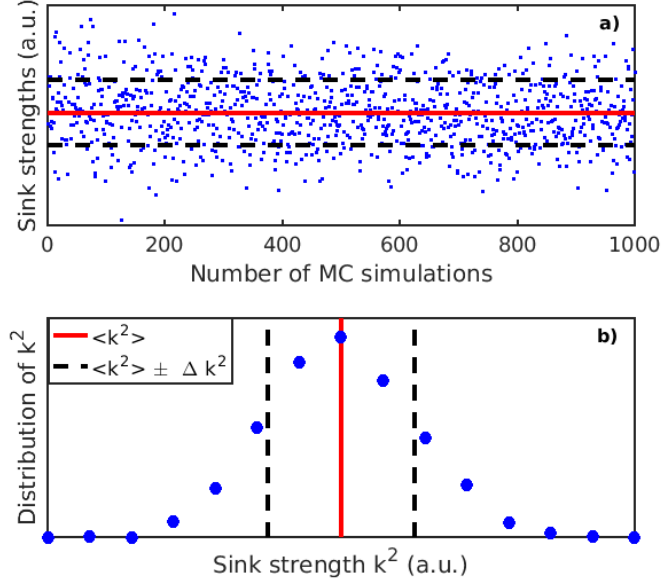


Figure A.9: **a)** The sink strengths for thousand different MC simulations with the same parameters and number of defects,  $M = 1000$ , for each simulation. **b)** The distribution density for the obtained sink strengths. Red lines show the mean sink strength calculated from Eq. (1) and the dashed lines show the standard deviation for the simulated sink strengths from Eq. (A.5). We see that the  $k^2$  distribution is indeed Gaussian, where about three points out of four are inside the error estimate.

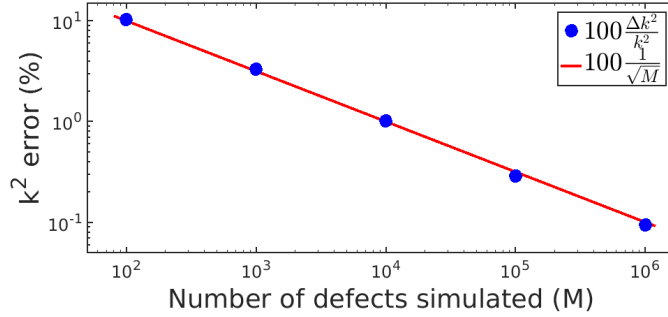


Figure A.10: The statistical error for the sink strength in percent as a function of the number of trapped defects simulated. The markers are calculated using Eq. (A.6), and the line using the simple rule in Eq. (A.7).

## Appendix B. Fast MC method to obtain the defect position after many diffusion jumps

The MC method of determining the sink strengths for systems with low trap volume fraction is very inefficient [7] due to the extremely large number of jumps a defect might diffuse before it finds a trap. To try to reduce the computational burden we look closer at the solution of the three dimensional diffusion equation:

$$\frac{dP(x, y, z, t)}{dt} = D \left[ \frac{d^2 P(x, y, z, t)}{dx^2} + \frac{d^2 P(x, y, z, t)}{dy^2} + \frac{d^2 P(x, y, z, t)}{dz^2} \right]. \quad (\text{B.1})$$

The solution to Eq. (B.1) with an initial (time  $t = 0$ ) delta function at origin  $P = \delta(r)$  (the defect is at the origin at time zero) is:

$$P(x, y, z, t) = \frac{\exp(-[x^2 + y^2 + z^2]/A)}{(\pi \cdot A)^{3/2}} = \frac{\exp(-r^2/A)}{(\pi \cdot A)^{3/2}}, \quad (\text{B.2})$$

where  $P$  is the normalized probability density, see Fig. B.11 a), for the diffusing defect ( $\int_0^\infty 4\pi r^2 P dr = 1$ ),  $A = 4Dt$ ,  $D$  is the diffusion coefficient,  $t$  the diffusion time and  $r = \sqrt{x^2 + y^2 + z^2}$  is the distance the defect has diffused from its initial position at time  $t = 0$ . The diffusion coefficient in a cubic lattice is  $D = 1/6 \cdot \lambda^2 \cdot \Gamma$ , where  $\lambda$  is the diffusion length and  $\Gamma$  the jump frequency ( $\Gamma = \nu \cdot \exp(-E_m/k_B T)$ ),  $\nu$  is the attempt frequency and  $E_m$  is the migration barrier). The number of diffusion jumps  $N^j = \Gamma t$ , gives an alternative way of expressing parameter  $A$  as:

$$A = 4Dt = 2/3 \cdot \lambda^2 \cdot N^j. \quad (\text{B.3})$$

The radial position probability for the defect after  $N^j$  jumps is given by:

$$F(r) = 4\pi r^2 \frac{\exp(-r^2/A)}{(\pi \cdot A)^{3/2}}, \quad (\text{B.4})$$

which is illustrated in Fig. B.11 b). The mean diffusion distance  $\langle r \rangle$  and its standard deviation  $SD$ , marked as lines in the figure, are given by Eqs. (B.7) and (B.8), respectively. To calculate the distribution moments of Eq. (B.4) we define the integral:  $E(r^n) = \int_0^\infty r^n \cdot F(r) dr$ , which for  $n = 0, 1, 2, 3, 4$  becomes:

$$E(r^0) = 1, \quad E(r^1) = 2(A/\pi)^{1/2}, \quad E(r^2) = 3A/2, \quad (\text{B.5})$$

$$E(r^3) = 4A^{3/2}/\pi^{1/2}, \quad E(r^4) = 15A^2/4. \quad (\text{B.6})$$

The distribution moments of Eq. (B.4) can now be calculated as:

$$\langle r \rangle = E(r^1) = 2(A/\pi)^{1/2} = \frac{4(Dt/\pi)^{1/2}}{\lambda} = \frac{\lambda(8N^j/[3\pi])^{1/2}}{\lambda} \quad (\text{B.7})$$

$$\begin{aligned} SD &= (E((r - \langle r \rangle)^2))^{1/2} = (E(r^2) - E(-2\langle r \rangle r) + E(\langle r \rangle^2))^{1/2} \\ &= (E(r^2) - 2\langle r \rangle E(r) + \langle r \rangle^2)^{1/2} = (E(r^2) - \langle r \rangle^2)^{1/2} \\ &= (A/2[3 - 8/\pi])^{1/2} = \frac{(2Dt[3 - 8/\pi])^{1/2}}{\lambda} = \frac{\lambda(N^j[1 - 8/(3\pi)])^{1/2}}{\lambda} \end{aligned} \quad (\text{B.8})$$

$$\text{Skewness} = E((r - \langle r \rangle)^3)/SD^3 = [E(r^3) - 3E(r^2)\langle r \rangle + 2\langle r \rangle^3]/SD^3 \quad (\text{B.9})$$

$$\text{Kurtosis} = E((r - \langle r \rangle)^4)/SD^4 = [E(r^4) - 4E(r^3)\langle r \rangle + 6E(r^2)\langle r \rangle^2 - 4\langle r \rangle^4]/SD^4. \quad (\text{B.10})$$

The probability that the defect has diffused a distance  $r$  from its initial position after  $N^j$  jumps is proportional to the integral of Eq. (B.4):

$$\text{Int}(r) = \int F(r) dr = \text{erf}(X^{1/2}) - 2/B \cdot r \cdot \exp(-X), \quad (\text{B.11})$$

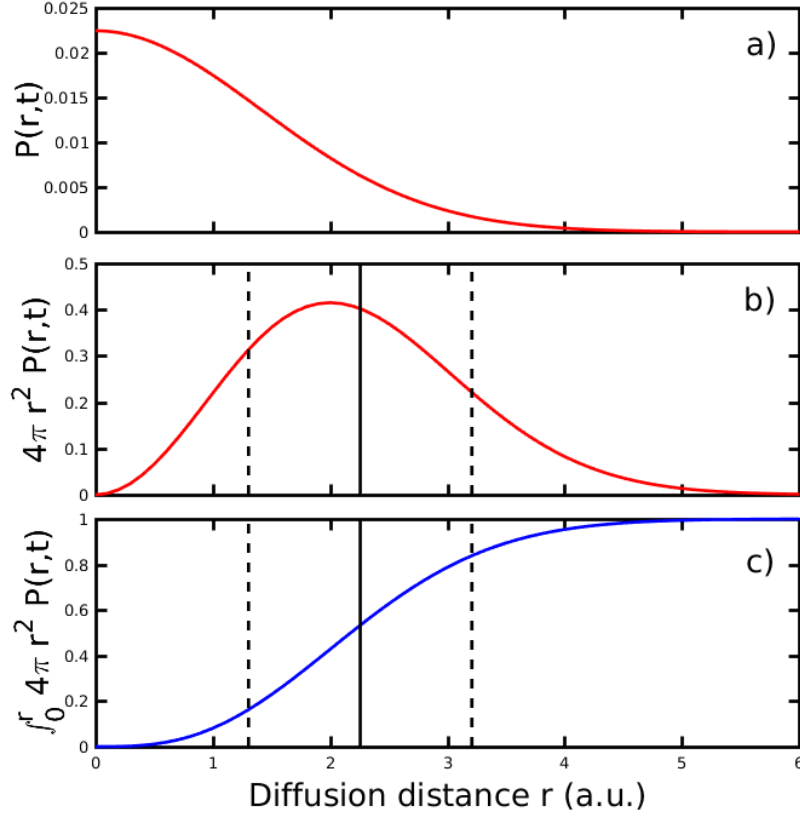


Figure B.11: a) The defect probability density function solution to the three dimensional diffusion equation. Initial defect position is at  $r = 0$ . b) The radial probability of the defect position after  $t$  seconds of diffusion. c) The probability integral as a function of diffusion distance  $r$ .

where  $X = r^2/A$ ,  $B = (\pi \cdot A)^{1/2}$ , and  $erf$  is the error function defined as:  $erf(y) = 2/\sqrt{\pi} \int_0^y exp(-t^2)dt$ . Figure B.11 c) shows the integral.

The aforementioned theory can now be used to calculate sink strengths faster as follows: we first place a defect in a random position in the simulation cell containing traps in random positions. We then check the closest distance ( $MinD$ ) for the defect to any trap. Thus, the defect cannot be trapped within  $N^j = floor(MinD/\lambda)$  diffusion jumps. We then use Eq. (B.11) with  $r_{max} = N^j \cdot \lambda$  to calculate the maximum integral value  $Int(r_{max})$ . We then generate a random number between 0 and  $Int(r_{max})$  and solve Eq. (B.11) for the corresponding diffusion distance  $r(N^j)$  for this defect after  $N^j$  jumps. To finally place the defect in a new place in three dimensions, we give further two random numbers to define a place with spherical coordinates  $[r(N^j), \theta, \phi]$ . The first one is the polar angle  $\theta$  from:  $cos(\theta) = 2 \cdot rand - 1$ , where the  $rand$  is a random number between 0 and 1. Secondly, we find the azimuthal angle:



$\phi = 2\pi \cdot rand$ , which gives the distances the defect is moved as:

$$\Delta x = r(N^j) \sin(\theta) \cos(\phi) \quad (\text{B.12})$$

$$\Delta y = r(N^j) \sin(\theta) \sin(\phi) \quad (\text{B.13})$$

$$\Delta z = r(N^j) \cos(\theta). \quad (\text{B.14})$$

To compare this approach to the usual MC method, where the defect makes  $N^j$  consecutive diffusion jumps, we simulated  $10^6$  defects that each make  $N^j = 10, 20, 50, 100, 200$  or  $500$  jumps with the jump length  $\lambda = 0.1$  nm and compare the diffusion distance distributions for the both methods. The  $N^j$  jumps were also tested with different diffusion jump directions:  $\langle 100 \rangle$ ,  $\langle 111 \rangle$  and random where the direction for the diffusing defect was chosen randomly. Figure B.12 illustrates the effect the number of jumps and jump direction has on the distance distribution for the defects.

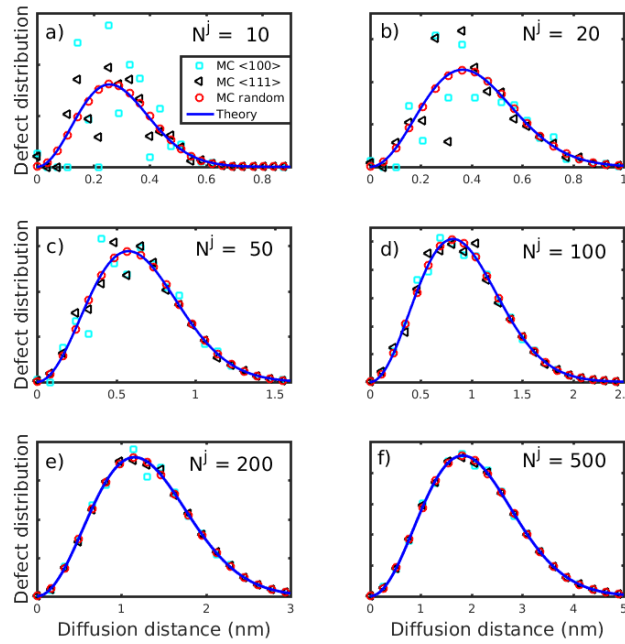


Figure B.12: The defect diffusion distributions with different number of jumps  $N^j$  obtained by usual MC simulations and present theory. The MC simulations were done with three different jump schemes, jumps in  $\langle 100 \rangle$ ,  $\langle 111 \rangle$  or random direction.

As can be seen, with  $N^j = 10$  jumps, the random direction jumps give about the same distance distribution as the theory Eq. (B.4). For jumps in the  $\langle 100 \rangle$  and  $\langle 111 \rangle$  directions, the  $N^j = 10$  jumps are not enough to obtain smooth distance distributions. When the number of jumps increase, the distance distributions with different jump directions all approach the theory as seen in Figure B.12 f) with  $N^j = 500$ . However, even if the distance distributions are not

exactly the same, the moments of the distributions are very close to each other already for smaller number of jumps as seen in Table B.1. We see that already for  $N^j$  over 20 jumps the present theory gives a good agreement with the MC method irrespectively of the jump direction. The advantage of the present theory is obvious from Figure B.12 f), where 500 consecutive diffusion jumps leads to a mean position change of only about 2 nm. The statistically same position change can now be made by generating one random number and using Eq. (B.11) to solve for the total diffusion distance. The obvious consequence using the new developed method is to substantially reduce the number of numerical calculations needed to make diffusion jumps until the defect is trapped, especially in a low trap volume fraction system where the distance to the closest trap is usually quite large.

There is, however, still one improvement to the developed method. Looking closer at Eq. (B.11), we see that the diffusion distance  $r$  cannot directly be solved, but has to be iterated numerically which can be time consuming. Fortunately there is a way of avoiding this: we can generate a uniformly spaced  $Int(r)$  grid and solve the corresponding  $r$ 's in advance. This makes another substantial reduction in the computational time when the diffusion distance can be deduced by simple uniformly spaced grid interpolation. The advantage of generating a  $Int(r)$  vs.  $r$  grid in advance is not obvious because Eq. (B.11) depends on both the present number of jumps  $N^j$  and the jump length  $\lambda$ . However, we can generate the  $Int(r)$  vs.  $r$  grid with any  $N^j$  and  $\lambda$ , and just scale the resulting diffusion distance with present number of jumps and jump length. To see how, the integral in Eq. (B.11) with  $N^j = N_1$  and  $\lambda_1$  becomes:

$$Int(r_1) = erf(X_1^{1/2}) - 2/B_1 \cdot r_1 \cdot exp(-X_1), \quad (B.15)$$

where  $X_1 = r_1^2/A_1 = 3r_1^2/(2\lambda_1^2N_1)$ , from Eq. (B.3), and  $B_1 = (\pi A_1)^{1/2} = (2/3\pi\lambda_1^2N_1)^{1/2}$ . If we now scale another diffusion distance  $r_2$  resulting from  $N_2$  and  $\lambda_2$  number of jumps and jump length, respectively, as:

$$r_2 = r_1 \frac{\lambda_2}{\lambda_1} \left( \frac{N_2}{N_1} \right)^{1/2}, \quad (B.16)$$

the integral with  $X_2 = 3r_2^2/(2\lambda_2^2N_2)$  and  $B_2 = (2/3\pi\lambda_2^2N_2)^{1/2}$  becomes:

$$Int(r_2) = erf(X_2^{1/2}) - 2/B_2 \cdot r_2 \cdot exp(-X_2) \quad (B.17)$$

$$= erf\left(\left[\frac{3r_2^2}{2\lambda_2^2N_2}\right]^{1/2}\right) - \frac{2r_2}{B_2} exp\left(-\frac{3r_2^2}{2\lambda_2^2N_2}\right) \quad (B.18)$$

$$= erf\left(\left[\frac{3r_1^2 \frac{\lambda_2^2 N_2}{\lambda_1^2 N_1}}{2\lambda_2^2 N_2}\right]^{1/2}\right) - \frac{2r_1 \frac{\lambda_2 N_2^{1/2}}{\lambda_1 N_1^{1/2}}}{(2/3\pi\lambda_2^2 N_2)^{1/2}} exp\left(-\frac{3r_1^2 \frac{\lambda_2^2 N_2}{\lambda_1^2 N_1}}{2\lambda_2^2 N_2}\right) \quad (B.19)$$

$$= erf\left(\left[\frac{3r_1^2}{2\lambda_1^2 N_1}\right]^{1/2}\right) - \frac{2r_1}{(2/3\pi\lambda_1^2 N_1)^{1/2}} exp\left(-\frac{3r_1^2}{2\lambda_1^2 N_1}\right) \quad (B.20)$$

$$= erf(X_1^{1/2}) - 2/B_1 \cdot r_1 \cdot exp(-X_1) = Int(r_1). \quad (B.21)$$

Thus we can generate a random number  $Int(r_1)$  and interpolate diffusion distance  $r_1$  calculated with  $N_1$  and  $\lambda_1$ . The right diffusion distance  $r_2$  with the present number of jumps  $N_2$  and  $\lambda_2$  is then obtained from Eq. (B.16). Visually this can be understood in such a way that the integral calculated with specific  $N_1$  and  $\lambda_1$  in Fig. B.11 c) will be exactly the same if we scale the diffusion distance  $r$  using Eq. (B.16) for another integral calculated with any  $N_2$  and  $\lambda_2$ . A similar idea to the method developed here is presented by Dalla Torre *et al.* [12], where defects perform macro-jumps whose distance is given by the continuous diffusion law. In their method the diffusion distance is calculated for a given time interval, whereas here it is related to the number of atomic jumps (specific to sink strength calculations). The time interval can also be used here by using Eq. (B.3) to relate the number of jumps to a time interval.

Table B.1: Comparison between defect diffusion distribution moments obtained by MC simulations and present theory, see Fig. B.12.  $\langle 100 \rangle$ ,  $\langle 111 \rangle$  and Random refers to results obtained by the MC method with different diffusion jump directions.

	$\langle r \rangle^a$ [nm]	SD <sup>b</sup> [nm]	Skewness <sup>c</sup>	Kurtosis <sup>d</sup>
$N^J = 10$				
$\langle 100 \rangle$	0.2921	0.1218	0.2467	2.9892
$\langle 111 \rangle$	0.2924	0.1202	0.3155	2.9660
Random	0.2928	0.1194	0.3687	2.8558
Theory	0.2913	0.1230	0.4857	3.1082
$N^J = 20$				
$\langle 100 \rangle$	0.4119	0.1722	0.4190	3.0437
$\langle 111 \rangle$	0.4129	0.1716	0.4201	3.0073
Random	0.4132	0.1715	0.4299	2.9841
Theory	0.4120	0.1739	0.4857	3.1082
$N^J = 100$				
$\langle 100 \rangle$	0.9203	0.3884	0.4772	3.0732
$\langle 111 \rangle$	0.9208	0.3876	0.4788	3.0884
Random	0.9217	0.3877	0.4746	3.0822
Theory	0.9213	0.3888	0.4857	3.1082
$N^J = 500$				
$\langle 100 \rangle$	2.0595	0.8692	0.4862	3.0976
$\langle 111 \rangle$	2.0605	0.8691	0.4832	3.1024
Random	2.0606	0.8694	0.4829	3.1038
Theory	2.0601	0.8694	0.4857	3.1082

<sup>a</sup>  $\langle r \rangle = \sum_i r_i D(r_i) / \sum_i D(r_i)$ , Eq. (B.7)

<sup>b</sup> SD =  $[\sum_i (r_i - \langle r \rangle)^2 D(r_i) / \sum_i D(r_i)]^{1/2}$ , Eq. (B.8)

<sup>c</sup> Skewness =  $[\sum_i (r_i - \langle r \rangle)^3 D(r_i) / \sum_i D(r_i)] / SD^3$ , Eq. (B.9)

<sup>d</sup> Kurtosis =  $[\sum_i (r_i - \langle r \rangle)^4 D(r_i) / \sum_i D(r_i)] / SD^4$ , Eq. (B.10)

### Appendix C. Analytical sink strength for spherical trap with volume correction

The sink strength for defects to a trap with concentration  $c_t$  from Brailsford and Bullough [6], (neglecting the thermal emission) is calculated by

$$k^2 = \frac{c_t \int_S (\vec{F} \cdot \vec{n}) dS}{D \langle c \rangle}, \quad (\text{C.1})$$

where  $\int_S (\vec{F} \cdot \vec{n}) dS$  is the flux of defects through the trap surface area,  $D$  is the defect diffusion coefficient and  $\langle c \rangle$  is the mean defect concentration in the system. If the trap shape is symmetric and the flux of defects to the trap boundary is constant from all directions  $|\vec{F}| = \text{constant}$ , we can write the surface integral, Eq. (C.1), simply as:

$$\int_S (\vec{F} \cdot \vec{n}) dS = |F| S, \quad (\text{C.2})$$

where  $S$  is the trap surface area. To find the analytical sink strength we choose a spherical volume with radius  $L$  with

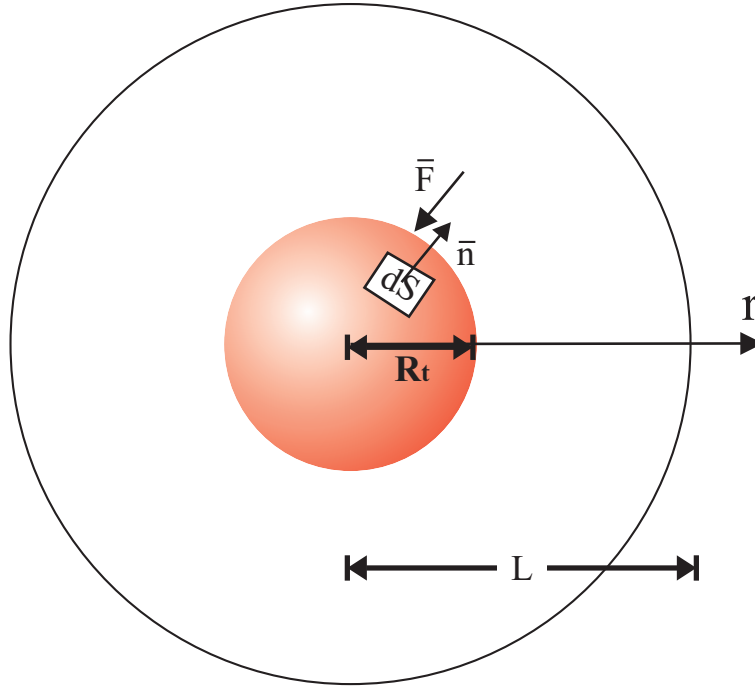


Figure C.13: The spherical cell with radius  $L$  with a spherical trap with radius  $R_t$  in the middle.

a spherical trap with radius  $R_t$  at the origin, see Fig. C.13. At time  $t = 0$  the defects starts to be produced in the whole volume (except the trap volume) with a production rate  $K$  [ $\text{m}^{-3}\text{s}^{-1}$ ]. A spherically symmetric defect concentration profile as a function of  $r$  from the trap edge and time  $t$  develops. This profile satisfies following equation in spherical coordinates

$$\frac{dc}{dt} = D \nabla^2 c + K = \frac{D}{r^2} \frac{\partial}{\partial r} \left( r^2 \frac{\partial c}{\partial r} \right) + K. \quad (\text{C.3})$$

The steady state differential equation to solve becomes:

$$0 = \frac{1}{r^2} \frac{\partial}{\partial r} \left( r^2 \frac{\partial c}{\partial r} \right) + \frac{K}{D}. \quad (\text{C.4})$$

The solution must give zero concentration of defects at the trap boundary  $r = R_t$ :  $c(R_t) = 0$ . Further, we assume a spherical simulation cell, where the flux of defects through the boundary at  $r = L$  is zero:  $\frac{\partial c}{\partial r}|_{r=L} = 0$ . The solution to the differential equation is:

$$c(r) = \frac{K}{3D} \left[ L^3 \left( \frac{1}{R_t} - \frac{1}{r} \right) + \frac{1}{2} (R_t^2 - r^2) \right]. \quad (\text{C.5})$$

The flux of defects at the trap boundary is:

$$|F| = D \frac{\partial c}{\partial r} |_{r=R_t} = D \frac{K}{3D} \left[ \frac{L^3}{R_t^2} - R_t \right]. \quad (\text{C.6})$$

The mean defect concentration for this spherically symmetric system becomes:

$$\langle c \rangle = \int_{V_m} c dV = \frac{\int_{R_t}^L c(r) 4\pi r^2 dr}{4\pi L^3/3} = \frac{3}{L^3} \int_{R_t}^L c(r) r^2 dr \quad (\text{C.7})$$

$$= \frac{K}{3D} \left[ \frac{L^3}{R_t} - \frac{9L^2}{5} + R_t^2 - \frac{1}{5} \frac{R_t^5}{L^3} \right]. \quad (\text{C.8})$$

The sink strength follows using definition in Eq. (C.1):

$$k^2 = \frac{c_t |F| S}{D \langle c \rangle} = \frac{c_t D \frac{K}{3D} [L^3/R_t^2 - R_t] 4\pi R_t^2}{D \frac{K}{3D} [L^3/R_t - 9L^2/5 + R_t^2 - R_t^5/(5L^3)]} \quad (\text{C.9})$$

$$= \frac{c_t [1 - R_t^3/L^3] 4\pi R_t}{[1 - 9R_t/(5L) + R_t^3/L^3 - R_t^6/(5L^6)]}. \quad (\text{C.10})$$

Note that if  $L \gg R_t$  we get the classical low trap concentration sink strength:  $k_i^2 \approx 4\pi R_t c_t$ . This equation is known as the Wiedersich formula [2, 3].

## References

- [1] P. M. Derlet, D. Nguyen-Manh, and S. L. Dudarev, *Phys. Rev. B* **76**, 054107 (2007).
- [2] H. Wiedersich, *Radiation Effects* **12**, 111 (1972).
- [3] F.A. Nichols, *J. Nucl. Mater.* **75**, 32 (1978).
- [4] G. Freeman, *Kinetics of nonhomogeneous processes*, L.K. Mansur: *Mechanisms and Kinetics of Radiation Effects in Metals and Alloys*. John Wiley and Sons, New York, NY, Jan 1987.
- [5] T. Ahlgren, K. Heinola, K. Vörtler, and J. Keinonen, *J. Nucl. Mater.* **427**, 152 (2012).
- [6] A. D. Brailsford and R. Bullough, *Philos. Trans. R. Soc. London* **302**, 87 (1981).
- [7] L. Malerba, C. S. Becquart, and C. Domain, *J. Nucl. Mater.* **360**, 159 (2007).
- [8] V. Jansson, L. Malerba, A. D. Backer, C. S. Becquart, and C. Domain, *J. Nucl. Mater.* **442**, 218 (2013).
- [9] H. Rouchette, L. Thuinet, A. Legris, A. Ambard, and C. Domain, *Comp. Mater. Sci.* **88**, 50 (2014).
- [10] J. Hou, X.-S. Kong, X.-Y. Li, X. Wu, C. Liu, J.-L. Chen, and G.-N. Luo, *Comp. Mater. Sci.* **123**, 148 (2016).
- [11] L. H. Heinisch, B. N. Singh, and S. I. Golubov, *J. Nucl. Mater.* **283–287**, 737 (2000).
- [12] J. Dalla Torre, J.-L. Bocquet, N. V. Doan, E. Adam, and A. Barbu, *Philos. Mag.* **85**, 549 (2005).